

*J. Nano- Electron. Phys.*  
3 (2011) No1, P.59-66

© 2011 SumDU  
(Sumy State University)

PACS numbers: 81.20.Fw, 81.07.Bc, 07.07.Df.

## SYNTHESIS AND CHARACTERIZATION OF Co-DOPED SnO<sub>2</sub>/TiO<sub>2</sub> SEMICONDUCTOR NANO CRYSTALLITES VIA SOL-GEL METHOD

**H.Z.R. Hamoon<sup>1</sup>, G.S. Devi<sup>1</sup>, H. Beigi<sup>2</sup>, J.V.R. Rao<sup>2</sup>, K.R. Reddy<sup>1</sup>, A. Nanaji<sup>1</sup>**

<sup>1</sup> Inorganic and Physical Chemistry division,  
Indian Institute of Chemical Technology,  
Tarnaka, Hyderabad, AP, India  
E-mail: [hedayatzadehamoon@yahoo.com](mailto:hedayatzadehamoon@yahoo.com)

<sup>2</sup> Center for Nano Science & Technology,  
Institute of Science and Technology, JNTUH,  
Kukatpally, Hyderabad, 500085, AP, India

*SnO<sub>2</sub>/TiO<sub>2</sub> nano particles are novel wide band gap semiconductors with modified applications of SnO<sub>2</sub> and TiO<sub>2</sub> in some fields including gas sensing, photo catalytic, solar cells and so on. The Co-doped SnO<sub>2</sub>/TiO<sub>2</sub> nano particles were obtained via sol-gel method with different amounts of doping material as 2.5 %, 6 % and 10 mol %. The crystallite sizes of resulting material were from 3.8 nm for 0.1 wt % Co-doped SnO<sub>2</sub>/TiO<sub>2</sub> to 19.1 nm for un-doped. Morphology and nanostructure of the crystalline SnO<sub>2</sub>/TiO<sub>2</sub> nano particles were characterized by means of X-ray diffraction, Raman spectroscopy, Fourier transform infrared spectroscopy (FTIR), Thermal gravimetric analysis (TGA), field emission scanning electron microscopy (FESEM) and energy dispersive X-ray spectroscopy (EDX). It has been shown that fine semiconductor nano structures were formed.*

**Keywords:** SnO<sub>2</sub>/TiO<sub>2</sub>, Co-DOPED, SEMICONDUCTOR, XRD, NANOPARTICLE.

(Received 04 February 2011, in final form 20 March 2011)

### 1. INTRODUCTION

SnO<sub>2</sub> is an opto electrical n-type semiconductor that has many interesting properties. These properties have made it a reliable material for gas sensing and catalysis applications [1, 2]. Even gas sensors based on SnO<sub>2</sub> materials are commercially available today [3]. SnO<sub>2</sub>-based nano powders and devices are obtained by means of a variety of synthesis techniques including the co precipitation [4], ion sputtering [5], microwave heating method [6], surfactants mediate [7,8], sol-gel methods [9] and so on.

On the other hand TiO<sub>2</sub> is also an n-type semiconductor that has been subject of many research studies in the last decade. It has been extensively employed in many applications mainly to photo catalytic decontamination treatments. [11-12].

One of the effective methods for obtaining desired material with modified properties is mixing two different semiconductors with appropriate conduction and valence band edges [13]. With coupling two metal oxide nanoparticles, better structures with more advantages for sensor applications can be achieved [14-15].

The energy levels of the valence and conduction bands are 3.7 eV and (ECB = 0 V versus NHE at pH 7) for SnO<sub>2</sub> and 2.7 eV (ECB = - 0.5 V versus

NHE at pH 7) for  $\text{TiO}_2$  [16, 17]. The band gap energy level of  $\text{SnO}_2$  is higher than that of  $\text{TiO}_2$ ; the conduction band of  $\text{SnO}_2$  is at a lower level than that of  $\text{TiO}_2$ 's. The higher reduction power of electrons and the higher oxidation power of holes correspond to the higher position of conduction band and the lower position of valence band, respectively. Therefore, mixing two semiconductors with different energy levels for their corresponding conduction and valence bands can provide an approach to achieve better applications by increasing the efficiency of charge separation, charge carrier lifetime, interfacial charge transfer rate and extending the energy range of photo excitation [16].

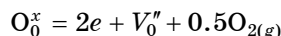
Mixed oxides can be formed in three ways along follow lines:

- (1) Chemical compound.
- (2) Solid solution
- (3) Mix of (1) and (2) types.

The  $\text{SnO}_2$ - $\text{TiO}_2$  mixture belongs to second category [18]. The  $\text{SnO}_2$ - $\text{TiO}_2$  coupled semiconductor commonly is synthesized by mixing the colloidal solutions of  $\text{SnO}_2$  and  $\text{TiO}_2$  [19, 20]. In recent years the properties of Co-doped  $\text{SnO}_2$  nanoparticles and Co-doped  $\text{TiO}_2$  nano particles have been exhaustively investigated. [21, 22, 23]

In the case of Co-doped  $\text{TiO}_2$  the main focus has been on the inherent ferromagnetism property of resulting nano structure at or above room temperature. Co:  $\text{TiO}_2$  nano particles are one of the most prominent diluted magnetic semiconductors (DMS) In the field of spintronics, especially for magneto-opto-electronic applications [24-25] DMSs have significant potential for future applications in the solar cells, biomedical and environmental fields. Co-doping  $\text{SnO}_2$  also has been widely studied [21]. One of the new emerging applications of  $\text{SnO}_2$  nano particles doped with Co is in varistor base materials.

$\text{SnO}_2$  with native oxygen vacancies compensated by electrons:



Using tin oxide ceramics is limited as dense ceramic since it is hard to make it denser because of evaporation and condensation, which enhance the grain growth, mostly dominate mass transport [26, 27]. Several sintering aids have been used to improve the densification of  $\text{SnO}_2$  ceramics [23, 28]. Recent reports suggest Co is used as sintering aids [23, 29].

Hence the investigation of nano particles of mix of  $\text{SnO}_2$ - $\text{TiO}_2$  doped via Co would have many advantages and it selected as a novel semiconductor for the current subject of this study. In this paper, a fine mixture nano-structural  $\text{SnO}_2$ - $\text{TiO}_2$  with different dosages of doped-Co is synthesized via sol-gel method while  $\text{SnCl}_4$  as a common precursor for producing  $\text{SnO}_2$  nano crystallite structure has been used. The mixture ratio of 3:1 has been kept constant for all samples and the Co doped amount varied from 0 % to 10 mol %. Geometry, particle size, morphology of nano crystallite structures are estimated by measurements.

## 2. EXPERIMENTAL WORK

Stannic chloride ( $\text{SnCl}_4$ , spectrochem Pvt. Ltd, Mumbai), titanium chloride ( $\text{TiCl}_4$ , spectrochem Pvt. Ltd, Mumbai), Poly Ethylene Glycol (6000LR, s-d fine-chem Limited, Mumbai), Ammonia solution 25% (Extra pure, s-d fine-

chem Limited, Mumbai) were purchased as precursors. 0.3 mol ( $\text{SnCl}_4$ ) and 0.1 mol  $\text{TiCl}_4$  were separately diluted using distilled water under simultaneous stirring condition for 45 min. 13 grams of PEG was dissolved in 300 ml distilled water and was stirred for 30 min until transparent solution was obtained. Diluted  $\text{SnCl}_4$  and  $\text{TiCl}_4$  were added drop by drop to the above solution simultaneously. Solution continued to remain under vigorous stirring for more than an hour. Appropriate amounts of  $\text{CoCl}_2$  for (0.25 mol %) Co-doping after dissolving in distilled water was added to mixture and was stirred for 30 min. 25 % aqueous ammonia solution was employed for adjusting PH value of the resulting solution to around 3. Then stirring condition was continued vigorously for one hour. The resulting sol was filtered and washed with distilled water and acetone twice, respectively, and dried overnight at 80 °C. Resulting solid was ground followed by calcination at 550 °C for 2 hours. This procedure was repeated three times with varying the amounts of  $\text{CoCl}_2$  addition for obtaining four different nano powders with 0%, 2.5%, 6%, 10 mol % Co-doped finally.

### 3. RESULTS

#### 3.1 TGA

Main Co-doped  $\text{SnO}_2/\text{TiO}_2$  (6 mol % doped) thermo gravimetric analysis (TGA) was accomplished in a flow of air with a temperature ramp of 50 °C/min and  $\alpha$ -alumina was used as the reference. Fig. 1 shows the weight loss (TG) and the differential thermo-analysis (DTA) curves corresponding to Co-doped  $\text{SnO}_2/\text{TiO}_2$  without any thermal annealing. The TG curve exhibits one endothermic weight loss at temperatures lower than 130 °C with 16.6 % weight loss that is associated with the loss of the residual water and trapped solvent in the particles. From 130 °C to 275 °C and 275 °C to 310 °C there are two small exothermic peaks corresponding to 6.6 % and 9.3 % relative weight losses respectively. About 360 °C a vigorous exothermic peak was observed accompanied by 9.3 % loss weight. Last exothermic peak at 500 °C corresponds to 6.6 weight loss. These exothermic peaks are likely due to decomposition of resulting nano crystallite structures, as confirmed by XRD analysis shown in Fig. 2. No more peak and no further weight loss observed in the TGA/DTA curves.

#### 3.2 XRD

Structural properties of all 0 %, 2.5 %, 6 %, 10 mol % Co-doped  $\text{SnO}_2/\text{TiO}_2$  samples were studied using X-ray diffraction (XRD: XRG 3000, Inel, France). The XRD results obtained were compared to the Joint Committee on Powder Diffraction Standards (JCPDS) X-ray data file. The crystallite size of the samples was calculated using the Scherrer formula:

$$T = 0.9\lambda/(\beta\cos\theta)$$

Where  $T$  is the particle size in nanometers,  $\lambda$  is the wavelength of Co radiation ( $\lambda = 1.78897$ ),  $\beta$  is the FWHM of the strongest peak and  $\theta$  is the peak position. By using the equation the crystal size of all different nanoparticles were calculated for each calcined temperature and are depicted

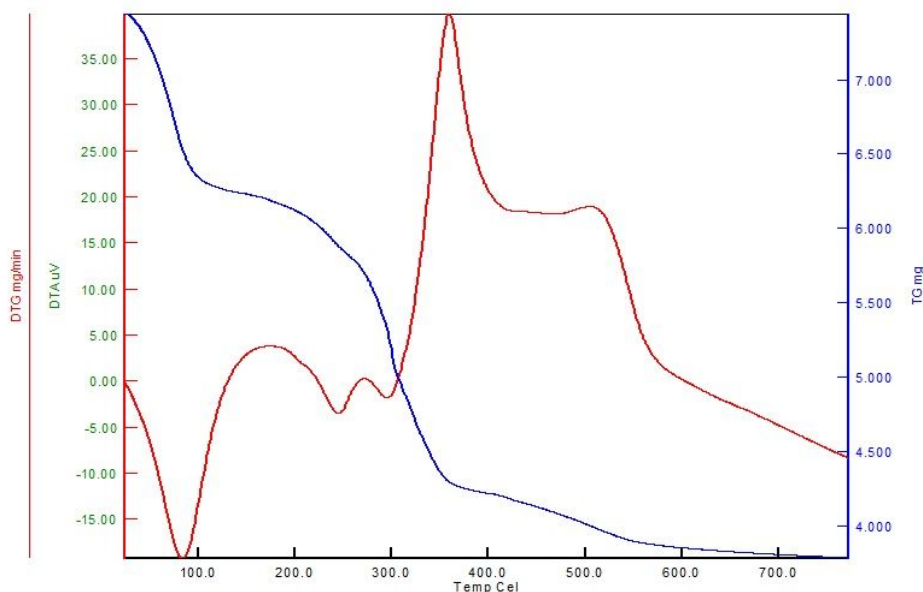


**Fig. 1** – TGA and DTA curves of Co-doped  $\text{SnO}_2/\text{TiO}_2$

in Table 1. Presence of  $\text{SnO}_2$  and rutile  $\text{TiO}_2$  were confirmed by PDF# 77-0451 (5 peaks are match) and PDF#76-0326 (2 peaks 111 and 211) respectively. Also CoO (hexagonal) peak was observed (PDF#89-2803 and peak 110). Decreasing the crystallite size is proportional with amount of Co-doped to  $\text{SnO}_2/\text{TiO}_2$ .

**Table 1** – Crystallite and particle size of Co-doped  $\text{SnO}_2/\text{TiO}_2$  nanostructures

Sample	Crystallite size (nm)	Particle size (nm)
Un-doped $\text{SnO}_2/\text{TiO}_2$	19.1	27
2.5 mol % Co-doped $\text{SnO}_2/\text{TiO}_2$	15.5	21
6 mol % Co-doped $\text{SnO}_2/\text{TiO}_2$	4.3	17
10 mol % Co-doped $\text{SnO}_2/\text{TiO}_2$	3.8	16

### 3.3 Raman

The Raman spectra of all samples were depicted in Fig. 3 and were compared with literature data [30, 31, 32]. For characterization the wave length  $633 \text{ cm}^{-1}$  was used for adjusting Raman apparatus (Labram Horibb yvon). Commercial CoO Raman spectra are shown in Fig. 3e, two peaks at  $648, 485 \text{ cm}^{-1}$ . The  $\text{SnO}_2$  peak about  $630 \text{ cm}^{-1}$  corresponding to  $A_{1g}$  mode, and two bands at  $773$  and  $472 \text{ cm}^{-1}$  corresponding to  $B_{2g}$  and  $E_g$  modes, respectively; this being in accordance with literature data.  $\text{TiO}_2$  rutile has peaks with following values:  $235, 447$  [30] or  $235, 447, 612$  [31].

Peaks of  $\text{TiO}_2$  rutile and  $\text{SnO}_2$  and CoO were confirmed and that is in agreement with other characterization data.

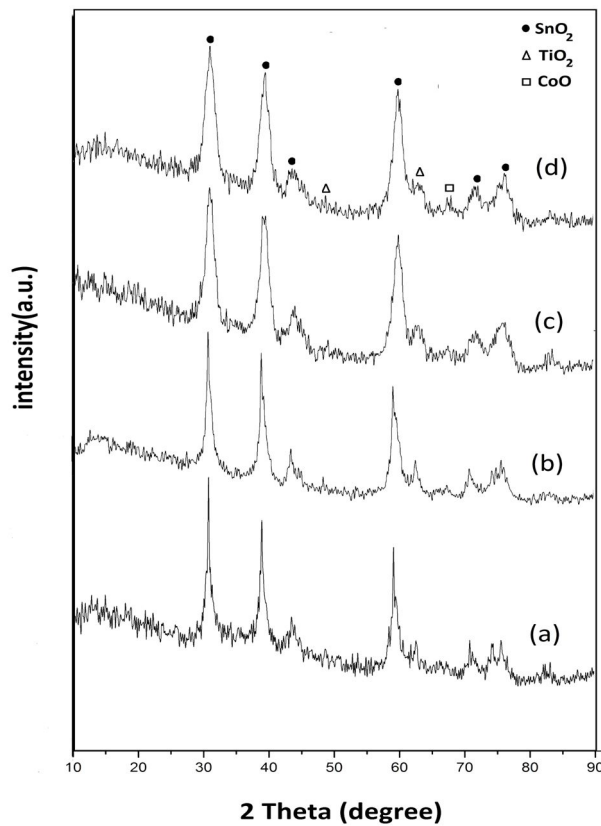


**Fig. 2** – XRD pattern of Co-doped SnO<sub>2</sub>/TiO<sub>2</sub> (a) un-doped (b) 2.5 mol % doped (c) 6 mol % doped (d) 10 mol % doped

### 3.4 FTIR

The FTIR analysis was carried out in order to determine the functional group of materials existed in Co-doped to SnO<sub>2</sub>/TiO<sub>2</sub> samples. The analysis was recorded using FTIR spectrometer (bruker) in a range between 4000 and 400 cm<sup>-1</sup>.

Fig. 4 shows the FTIR spectra of Co-doped to SnO<sub>2</sub>/TiO<sub>2</sub>. The bands at 3543 - 3393 cm<sup>-1</sup> correspond to the O-H mode of vibration [33]. The broad O-H peaks become narrower with an increase Co-doped amount, 3380 and 3050 cm<sup>-1</sup>, which may be due to the adsorbed water and NH. The N-H band observed around ca. 3050 cm<sup>-1</sup> may be due to the use of ammonia to promote SnCl<sub>4</sub> and TiCl<sub>4</sub> hydrolysis, which leads to the formation of ammonia. The strong asymmetric stretching mode of vibration of C = O was observed between 1668 cm<sup>-1</sup>. The symmetric stretching occurs between 1400 and 1334cm<sup>-1</sup> because of the presence of C-O. The C-O-C peak is present about 1070 cm<sup>-1</sup>. According to Du et al. [34], the C-O-C peak usually appears at 1256 cm<sup>-1</sup>. The absorption peaks at 1359, 1343, 1280, 1240, 1149 and 1077 cm<sup>-1</sup> result from the bending vibration of the O-H bond and stretching vibration of the C-O bond of the -CH<sub>2</sub>-OH group. In fact the XRD and EDX analysis proved that the synthesized powders in this work are Co-doped to SnO<sub>2</sub>/TiO<sub>2</sub> with the good stoichiometric composition.

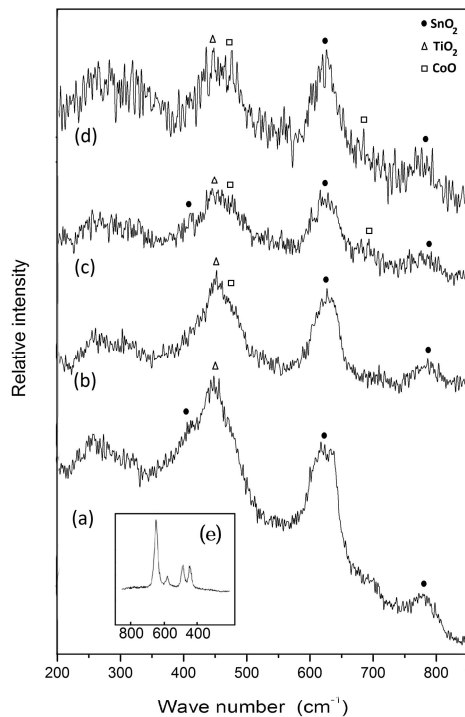


**Fig. 3** – Raman spectra of Co-doped  $\text{SnO}_2/\text{TiO}_2$  un-doped (a), 2.5 mol % doped (b), 6 mol % doped (c), 10 mol % doped (d), and commercial CoO (e)

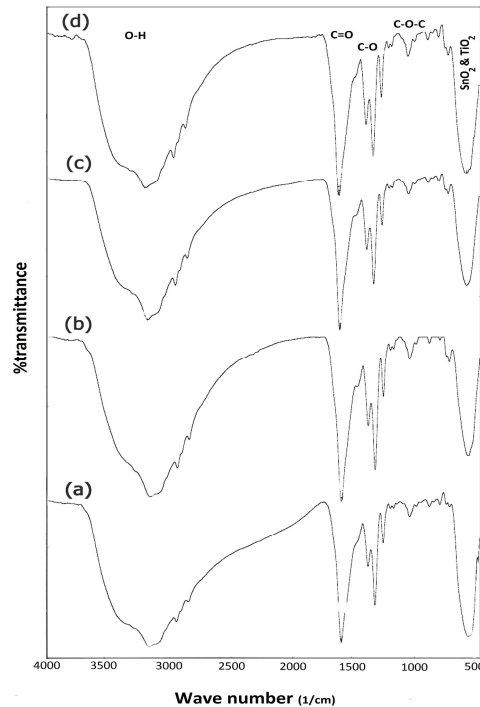


**Fig. 4** – FT-IR spectra of Co-doped  $\text{SnO}_2/\text{TiO}_2$  un-doped (a), 2.5 mol % doped (b), 6 mol % doped (c), and 10 mol % doped (d)

The particle size caused a large shift in the IR peak. The  $\text{SnO}_2$  peak that appears  $660\text{ cm}^{-1}$  shows that formation of tin oxide was completed. The FTIR results support the RAMAN, XRD, FESEM results.

### 3.5 FESEM

The surface morphology, particles size and composition of Co-doped to  $\text{SnO}_2/\text{TiO}_2$  nanoparticles were investigated by field emission scanning electron microscopy (FESEM) and energy dispersive X-ray spectroscopy (EDX). FESEM and EDX images of Co-doped to  $\text{SnO}_2/\text{TiO}_2$  powder nanoparticles are shown in Fig. 5. Nano particles with relatively high agglomeration are shown in Fig. 5 a and b. This agglomeration is a result of the acidic sols during the synthesis process. The particle sizes were estimate for all samples using images Table 1.

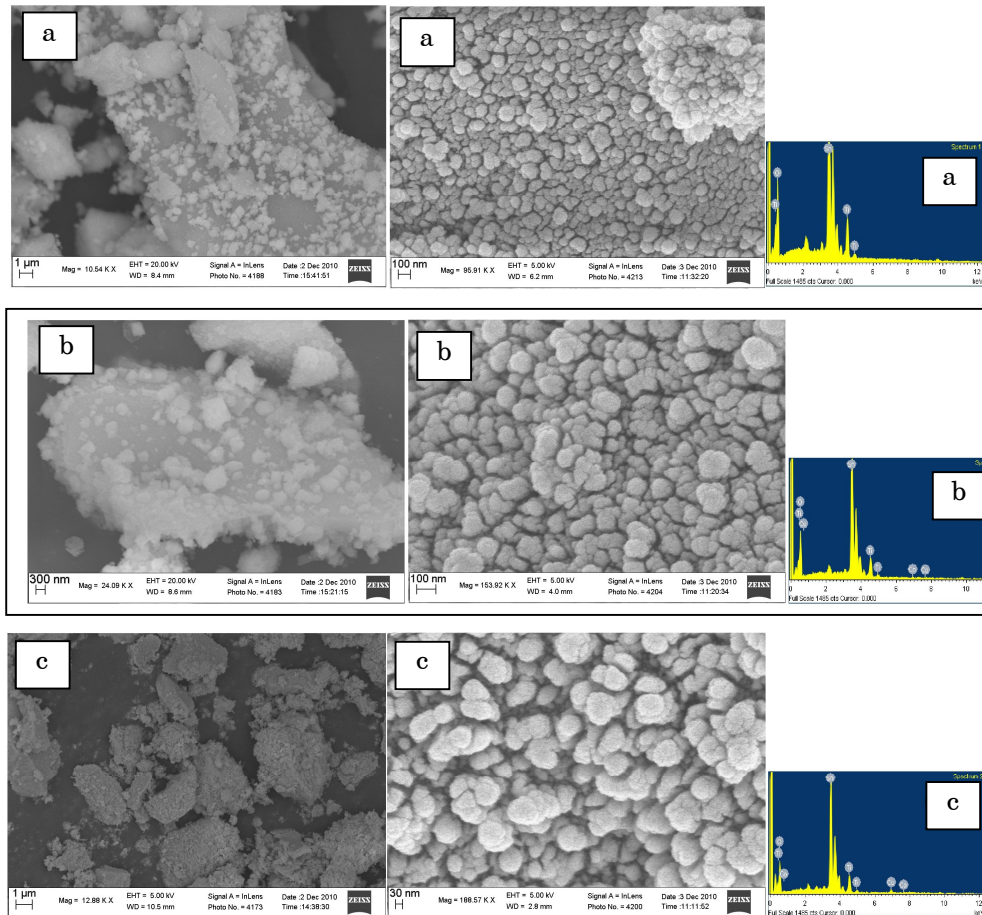


**Fig. 5** – FESEM and EDX images of Co-doped to  $\text{SnO}_2/\text{TiO}_2$  un-doped (a) 2.5 mol % doped (b) 10 mol % doped (c)

#### 4. CONCLUSION

A modified sol-gel process was designed to prepare Co-doped to  $\text{SnO}_2/\text{TiO}_2$ . The products were characterized by means of X-ray diffraction, Raman spectroscopy, Fourier transform infrared spectroscopy (FTIR), Thermal gravimetric analysis (TGA), field emission scanning electron microscopy (FESEM) and energy dispersive X-ray spectroscopy (EDX). Crystallite and particle size of the nano structures were decreased from 19.1 to 3.8 nm and 27 to 16 respectively by the addition of Co to the precursor solution. Fine Co-doped to  $\text{SnO}_2/\text{TiO}_2$  nano particles were obtained and applications were discussed.

#### ACKNOWLEDGEMENT

Hamoon H.Z.R. thanks Director IICT for permitting him to carry out his thesis work at IICT. A. Nanaji and Ravindranath Reddy thank CSIR and UGC for research fellowship.



## REFERENCES

1. M. Batzill, U. Diebold, *Prog. Surf. Sci.* **79**, 47 (2005).
2. M. Tiemann, *Chem. Eur. J.* **13**, 8376 (2007).
3. Microsens Inc. (<http://www.microsens.ch>).
4. A. Mosquera, J.E. Rodríguez-Pérez, J.A. Varela, P.R. Bueno, *J. Eur. Ceram. Soc.* **27**, 3893 (2007).
5. M. Ruske, G. Brauer, J. Pistner, U. Pfafflin, J. Szczyrbowski, *Thin Solid Films* **351**, 146 (1999).
6. J.-J. Zhu, J.-M. Zhu, X.-H. Liao, J.-L. Fang, M.-G. Zhou, H.-Y. Chen, *Mater. Lett.* **53**, 12 (2002).
7. J. Pal, P. Chauhan, *Mater. Charact.* **60**, 1512 (2009).
8. C. Liang, Y. Shimizu, T. Sasaki, N. Koshizaki, *J. Phys. Chem. B* **107**, 9220 (2003).
9. A. Kurz, K. Brakecha, J. Puetz, M.A. Aegerter, *Thin Solid Films*. **502**, 212 (2006).
10. N. Negishi, T. Iyoda, K. Hashimoto, A. Fujishima, *Chem. Lett.* **9**, 841 (1995).
11. I. Sopyan, M. Watanabe, S. Murasawa, *Chem. Lett.* **1**, 69 (1996).
12. A.L. Linsebigler, G.Q. Lu, J.T. Yates, *Jr. Chem. Rev.* **95**, 735 (1995).
13. J. Shang, W. Yao, *Appl. Catal. A-Gen* **257**, 25 (2004).
14. K. Zakrzewska, *Thin Solid Films* **391**, 229 (2001).
15. P. Nelli, L.E. Depero, M. Ferroni, S. Groppelli, V. Guidi, F. Ronconi, L. Sangaletti, G. Sberveglieri, *Sens. Actuat. B Chem.* **31**, 89 (1996).
16. O. Carp, C.L. Huisman, A. Reller, *Prog. Solid State Chem.* **32**, 33 (2004).
17. K. Vinodgopal, P.V. Kamat, *Environ. Sci. Technol.* **29**, 841 (1995).
18. N.V. Duy, N.V. Hieu, *Physica E* **41**, 258 (2008).
19. P.V. Kamat, *Chem. Rev.* **93**, 267 (1993).
20. I. Bedja, S. Hotchandani, P.V. Kamat, B. Bunsen-Ges, *Phys. Chem. Chem. Phys.* **101**, 1651 (1997).
21. R. Parra, L.A. Ramajo, *Mater. Res. Bull.* **43**, 3202 (2008).
22. K.A. Griffin, A.B. Pakhomov, *Phys. Rev. Lett.* **94**, 157204 (2005).
23. R. Metz, D. Koumeir, J. Morel, J. Panisot, M. Houabes, M. Hassanzadeh, *J. Eur. Ceram. Soc.* **28**, 829 (2008).
24. H. Ohno, *Science* **281**, 951 (1998).
25. S.J. Pearton, W.H. Heo, M. Ivill, D.P. Norton, T. Steiner, *Semicond. Sci. Technol.* **19**, 59 (2004).
26. C. Li, J. Wang, W. Su, H. Chen, W. Zhong, P. Zhang, *Ceram. Int.* **27**, 655 (2001).
27. T. Kimura, S. Inada, T. Yamaguchi, *J. Mater. Sci.* **24**, 220 (1989).
28. J.A. Varela, O.J. Whittemore, E. Longo, *Ceram. Int.* **16**, 177 (1990).
29. S.A. Pianaro, P.R. Bueno, E. Longo, J.A. Varela, *J. Mater. Sci. Lett.* **14**, 692 (1995).
30. V.N. Kuznetsov, N. Serpone, *J Phys. Chem. B.* **110**, 25203 (2006).
31. T. Hirata, K. Ishioka, M. Kitajima, H. Doi, *Phys. Rev. B.* **53**, 8442 (1996).
32. Y. Liu, M. Liu, *Adv. Funct. Mater.* **15**, 57 (2005).
33. D.M. Fernandes, R. Silva, A.A.W. Hechenleitner, E. Radovanovic, M.A.C. Melo, E.A.G. Pineda, *Mater. Chem. Phys.* **115**, 110 (2009).
34. H. Du, F. Yuan, S. Huang, J. Li, Y. Zhu, *Chem. Lett.* **33**, 770 (2004).